Provided for non-commercial research and education use.
Not for reproduction, distribution or commercial use.

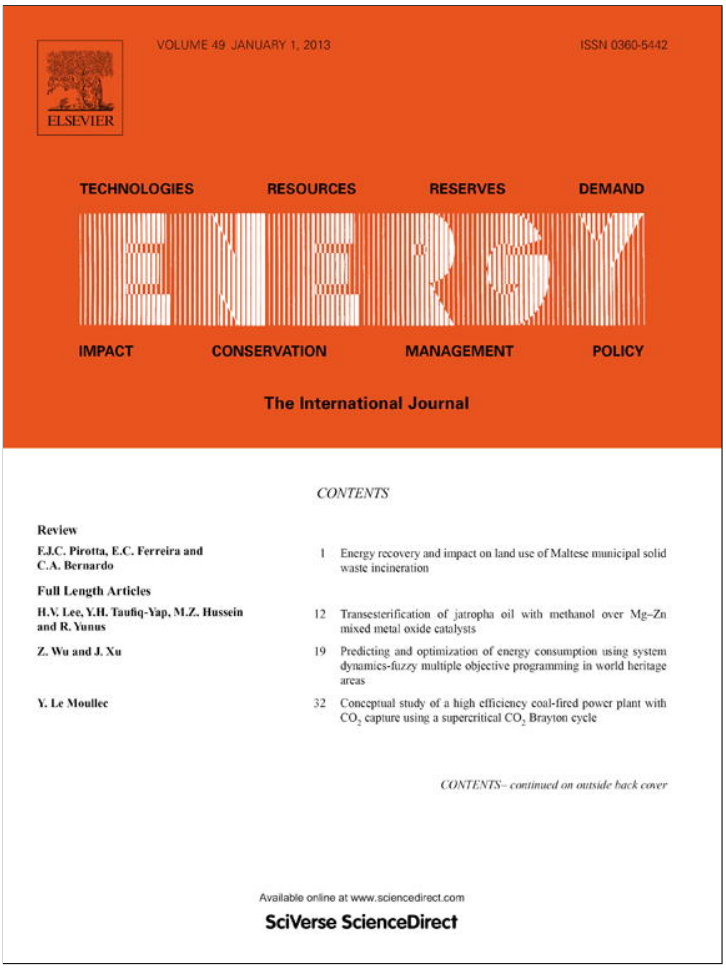

This article appeared in a journal published by Elsevier. The attached copy is furnished to the author for internal non-commercial research and education use, including for instruction at the authors institution and sharing with colleagues.

Other uses, including reproduction and distribution, or selling or licensing copies, or posting to personal, institutional or third party websites are prohibited.

In most cases authors are permitted to post their version of the article (e.g. in Word or Tex form) to their personal website or institutional repository. Authors requiring further information regarding Elsevier's archiving and manuscript policies are encouraged to visit:

http://www.elsevier.com/copyright

Author's personal copy

Energy 49 (2013) 146–155

Contents lists available at SciVerse ScienceDirect

Energy

journal homepage: www.elsevier.com/locate/energy

Design optimization of single mixed refrigerant natural gas liquefaction process using the particle swarm paradigm with nonlinear constraints

Mohd Shariq Khan, Moonyong Lee*

School of Chemical Engineering, Yeungnam University, Gyeongsan 712-749, South Korea

ARTICLE INFO

Article history:
Received 16 March 2012
Received in revised form
19 November 2012
Accepted 20 November 2012
Available online 20 December 2012

Keywords:
Single mixed refrigerant process
Particle swarm paradigm
Nonlinear constrained optimization
Natural gas liquefaction
Rigorous simulation
LNG

ABSTRACT

The particle swarm paradigm is employed to optimize single mixed refrigerant natural gas liquefaction process. Liquefaction design involves multivariable problem solving and non-optimal execution of these variables can waste energy and contribute to process irreversibilities. Design optimization requires these variables to be optimized simultaneously; minimizing the compression energy requirement is selected as the optimization objective. Liquefaction is modeled using *Honeywell UniSim Design*™ and the resulting rigorous model is connected with the particle swarm paradigm coded in MATLAB. Design constraints are folded into the objective function using the penalty function method. Optimization successfully improved efficiency by reducing the compression energy requirement by *ca.* 10% compared with the base case.

© 2012 Elsevier Ltd. All rights reserved.

1. Introduction

The liquefaction of natural gas (NG) is energy intensive and accounts for *ca.* 30% of the total energy used in NG processing. Several processes are available for baseload liquefied natural gas (LNG) plants, varying in complexity, capacity and efficiency. Single mixed refrigerant (SMR) liquefaction process has been reported as suitable for offshore LNG plants [1] also known as stranded natural gas plant [2]. It's simple design, ease of operation and small footprint make it cost effective for offshore NG fields developments [3]. Improving this process thermal efficiency can result in substantial cost and energy savings. Designing SMR processes often involves multivariable problem solving and much energy is wasted due to non-optimal execution of these variables, contributing to process irreversibilities. Optimal design requires decision variables to be optimized simultaneously. However the complex thermodynamics and nonlinear interactions between the variables make optimization a complex nonlinear, non-convex problem with many local optima.

Several approaches have been developed for optimizing mixed refrigerant systems. Initially the focus was on general refrigeration system and the earliest attempt at general MR system optimization is attributed to Ait Ali [4], whose two-dimensional numerical search was performed to find key trade-offs of the system including MR composition. Although sufficient insight into the MR system was developed, an ideal solution assumption and other thermodynamic shortcuts limit the practical application of this method. The search for environmentally friendly refrigerant mixtures was considered by Duvedi and Achenie [5], and an MINLP model was solved with an outer approximation algorithm to design a general MR system with desired properties. Considering a similar approach, Churi and Achenie [6] optimized a two-evaporator MR system with MINLP. Both of these approaches used sophisticated MINLP solvers with a compromised non-rigorous model, leading to a lack of confidence in the optimization results. Convergence of the MINLP problem is another issue. Vidyaraman and Maranas [7] conducted an optimization of horizontal and vertical cascade cycles of general MR system. Although the approach was comprehensive, but the assumption about no pressure drop in heat exchangers is unrealistic moreover, the assumption about MR stream entering at dew point temperature in compressor can potentially harm its blades. In another approach, Lee et al. [8] optimized the PRICO process. They analyzed three different objective functions, and the selection of compression energy minimization as objective was made through manual engineering judgments. A feasibility check was also performed manually, and this renders the approach more heuristic and dependent on the insight of practitioners. The use of nonlinear programming to solve complex thermodynamic problem also give

* Corresponding author. Tel.: +82 53 811 3262.
E-mail address: mynlee@yu.ac.kr (M. Lee).

0360-5442/$ – see front matter © 2012 Elsevier Ltd. All rights reserved.
http://dx.doi.org/10.1016/j.energy.2012.11.028

Author's personal copy

less confidence in optimization results. Mokarizadeh et al. [9] and Nogal et al. [10] also considered the optimization of the SMR process with genetic algorithm. Mokarizadeh et al. used a simplified model and thermodynamic calculations were not performed in commercial simulator. This renders the model less rigorous in comparison to models developed in commercial rigorous process simulators such as *Honeywell Unisim Design*™ adopted in this paper. Nogal et al. invested most efforts in developing a simplified model and optimization algorithm was not presented to understand what specific objective function they employed. Khan et al. [11] and Aspenlund et al. [12] also performed the optimization of SMR process under optimization-simulation framework. Khan et al. used a deterministic search method that can easily be lost in a multi local optimum problem. Aspelund et al. on contrary focused on different optimization tools and programs rather than the characteristics of the SMR process and the optimization approach lacks generality.

From the above discussion it is clear that most approaches adopt simplified models for sophisticated optimization. However, accurate optimal conditions are hardly obtained using models with compromised rigorousness or accuracy. Problems with convergence and local minima also remain obstacles to optimization using MINLP or NLP solvers. A balance between optimization methodology and modeling approach towards attaining optimal SMR plant design and operation was seriously needed and addressed in the current study. Non-traditional stochastic optimization techniques that employ most rigorous models for better optimization have been investigated. The particle swarm paradigm (PSP) is one such techniques and investigated for the optimization of SMR NG liquefaction process. The main objectives of this work are to minimize energy consumption as an objective function directly linked to the key decision variables and to demonstrate the effectiveness of PSP in optimization-simulation framework problems, using SMR NG liquefaction as an example. This work's approach is based on the optimization-simulation framework [12] that allows rigorous process models to be directly optimized through connection to a coded optimization routine. The SMR liquefaction process was first rigorously modeled using a commercial simulator, *Honeywell UniSim Design*™, and the developed model was connected with a PSP algorithm coded in MATLAB using COM functionality. The automation potential of the process simulator was exploited to run the PSP algorithm. Connection was smooth and the information exchanges between programs were seamless. The optimization results were also reported using case studies.

2. The particle swarm paradigm

The PSP is a non-calculus based method and can solve discontinuous, multi-modal, non-convex problems developed by Kennedy, J and Eberhart R.C [13]; PSP is attractive because of its few adjusting parameters and works well in a wide variety of applications, including evolving artificial neural networks, diagnosing human tumors [14], developing numerically-controlled machine tools [15] and optimizing reactive power and voltage control systems [16]. Energy resources management scheduling in smart grid [17], optimum design of solar air heater [18]. Process system design, explored here, potentially benefits greatly from the use of the PSP [19]. The PSP uses populations called particles or agents. These particles move around in the search-space, which is often multi-dimensional according to a few simple rules described by Eqs. (1) and (2). The PSP algorithm used in this study is illustrated in Fig. 1. The PSP algorithm starts by generating random positions for the particles within an initialization region. Particle velocities are usually initialized to prevent them from leaving the search space during the first iteration. During the main loop, the positions and velocities of the particles are iteratively updated until a stopping

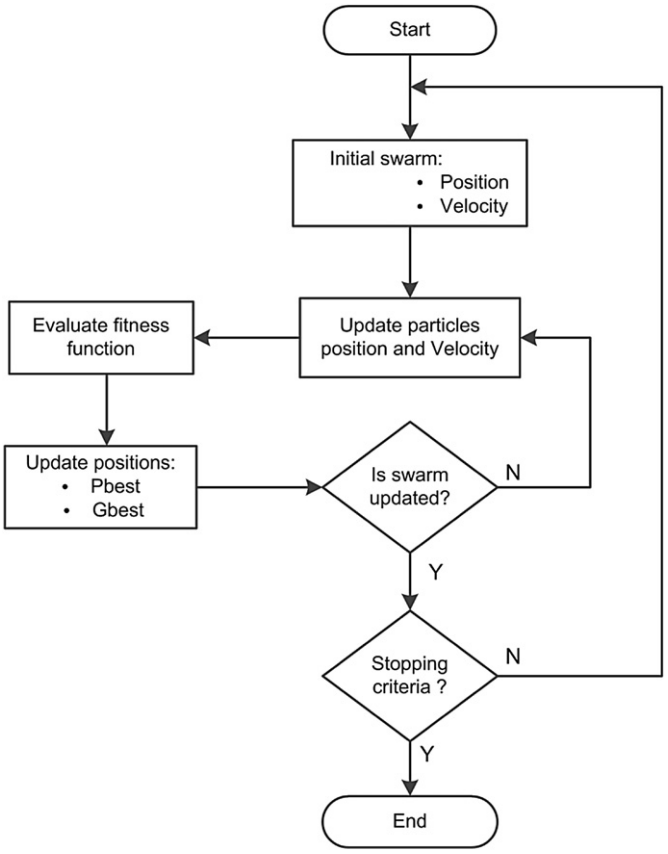

Fig. 1. PSP used algorithm.

criterion is met. Through iteration, each particle tracks the best solution (fitness) it has achieved, which the other particles can assess. By benefiting from the discoveries of the other particles, the whole swarm can more easily find the best position.

$$V_{i+1} = wV_i + c_1 r_1 (pBest_i - X_i) + c_2 r_2 (gBest_i - X_i) \quad (1)$$

$$X_{i+1} = X_i + V_{i+1} \quad (2)$$

Eq. (1) calculates a new velocity V_{i+1} for each particle based on its previous velocity, its best achieved location *pBest* and the best global location *gBest*. Eq. (2) updates individual particle's positions X_i in solution hyperspace. The two random numbers r_1 and r_2 are independently generated within the range [0,1]. The cognition and social parameters c_1 and c_2 in Eq. (1) represent the stochastic weighting terms, represents the confidence of an individual particle and of the swarm. Adjustment of these constants changes the amount of tension in the system. Low values allow the particle to roam far from target regions before being pulled back, while high values result in abrupt movement around target regions. The particles' velocities, on the other hand, are clamped in each dimension to a maximum velocity called *V*max. *V*max is an important parameter that determines the resolution or fitness with which the regions between the particles' present and target positions are searched, and restricts particle movement within the search space. To decrease the particle velocity linearly near optimum, the inertial weighting parameter *w* is used. The particle population is also an important factor for successful convergence of the PSP algorithm. Populations of around 20–50 are most common, and are optimal in terms of minimizing the total number of evaluations needed to obtain a good solution.

Author's personal copy

3. SMR process design

3.1. Process description

SMR liquefaction process was first installed in Skikda Algeria, licensed by Pritchard [20]. It is a simple NG liquefaction process using a multi-component mixture as a working fluid. In this study, the SMR process is modeled in *Honeywell UniSim Design*™ [21] which is one of the most widely used powerful rigorous commercial simulators for chemical plants and oil refineries. Its strong thermodynamic libraries, robustness in property calculations, user-friendly interface design and integrated steady state and dynamic modeling capabilities make this software well known in the chemical engineering industry and academia, especially for upstream, gas processing calculations and cryogenic facilities. A schematic diagram of the SMR process is outlined in Fig. 2. Note that in Fig. 2, different states are used for the description of the SMR process and will be referred to in the text as '*state-x*' ($x = 0, 1, 2\ldots$). NG enters the LNG exchanger at elevated pressure and ambient temperature (*state-0*). Heat is exchanged with the MR and leaves the exchanger in a sub-cooled state (*state-6*). NG is further flashed to atmospheric pressure in the JT valve and liquefied completely (*state-7*). After being compressed and cooled (*state-3*), MR is vaporized in the LNG exchanger and leaves in a superheated state (*state-4*). Lowering in pressure of MR stream in the JT valve decreases its temperature to −155 °C (*state-5*). Finally, MR is vaporized inside the heat exchanger and leaves in a superheated state (*state-1*) for further recompression. The NG-LNG stream (*pass 0-6-7*) and warm refrigerant (*pass 3-4*) are combined in a hot composite curve, while the cold refrigerant (*pass 5-1*) alone forms the cold composite curve (see Section 4.2). Usually, the heat transfer associated with LNG processes has an approach temperature as small as 1–3 °C [22]. In this study, the minimum internal temperature approach (MITA) value of 3 °C [23] was enforced.

3.2. LNG exchanger model in simulator

The multi-stream cryogenic LNG exchanger is a plate and fin-type apparatus brazed with an aluminum core. The temperature distribution of three streams in the LNG exchanger (NG feed, high and low pressure MR streams) can be calculated from the difference equations for local energy balance of each interval. The LNG exchanger in the *Unisim Design*™ rigorously solves heat and material balances for multi-stream heat exchangers based on the following general energy balance for each layer [21].

$$m'(h_{in} - h_{out}) + Q_{int} + Q_{ext} = 0 \tag{3}$$

where m', h_{in}, h_{out}, Q_{int} *and* Q_{ext} denote the fluid flow rate in the layer, specific enthalpy at the layer inlet and outlet, and heat gained from the surrounding layers and external environment, respectively.

The solution method can handle a wide variety of specified and unknown variables, like heat leak/loss, UA, or temperature approaches. Two solution approaches are employed: in the case of multiple unknowns, an iterative approach is used to satisfy both energy balance and any constraints while in the case of a single unknown the solution is calculated directly from an energy balance [21].

For the present study, the following hypotheses were used for the LNG exchanger model:

- Heat losses to environment are ignored.
- The pressure drop in heat exchanger is 1 bar for each stream.
- The temperature difference between the hot and cold streams of the heat exchanger must meet MITA value of 3 °C to ensure the validity of heat transfer.
- The heating curves are decomposed of sufficient number of intervals and the UA values are calculated for every interval and summed to calculate the overall exchanger UA.

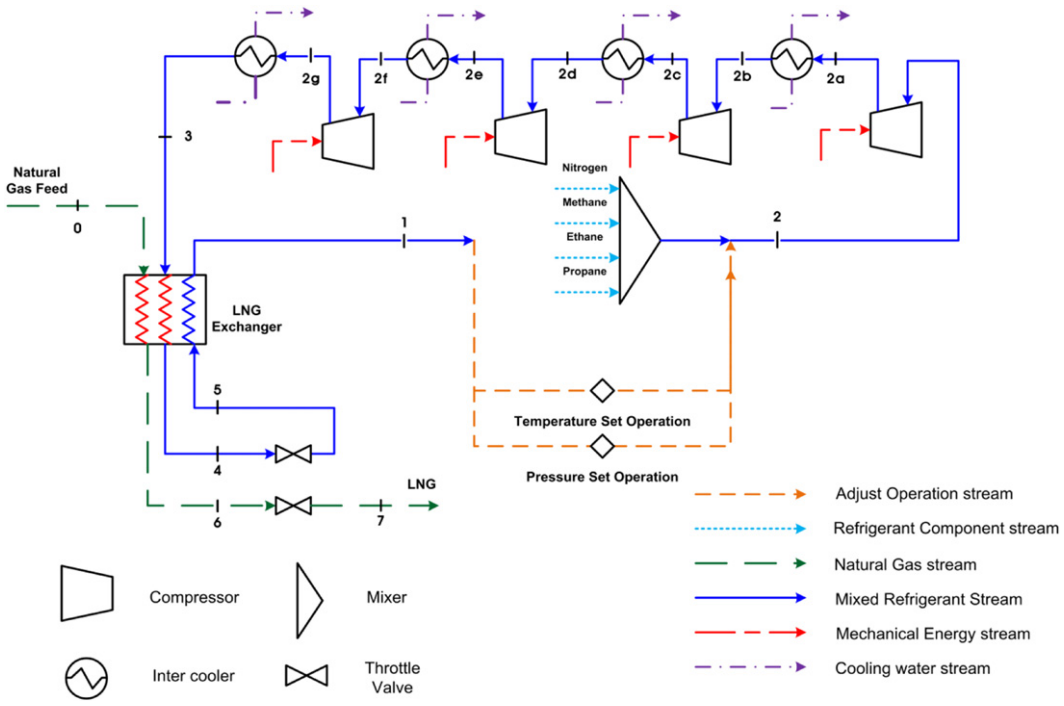

Fig. 2. Schematic diagram of SMR process.

Author's personal copy

3.3. Multi-staged compression and intercooling

In industry, it is very common to find that the compression task is performed in multiple stages. In this study, one dedicated compressor (centrifugal type) with four stages was used. The intermediate compressor in each stage shares a single-power driving axis, and the compression ratios between each stage are fixed evenly based on the optimized total compression ratio and thus not considered as independent optimizing variables. However, allowing dissimilar pressure ratios would mean more degree of freedom during optimization and bring more improvement to the MR system. The partially compressed MR is cooled in the intercooler (Fig. 2) to reduce its volumetric flow rate, and consequently, the compression power of the next stage. Compressors need a mechanical energy stream and are the main source of energy consumption in an SMR plant. Whereas in intercoolers, water is circulated as a thermal energy stream and the only consumption of energy is in pumping water, which is inherently much cheaper than gas compression and thus can be negligible. Inter-staged cooling was assumed to be performed with seawater, and an exit temperature limit of 40 °C was imposed. To bring more improvement in the compression energy requirement, refrigeration might be used for intermediate cooling. However, refrigeration provides an overall increase in the energy requirement of the SMR plant and conflicts with the main objective so must be avoided.

3.4. Compressor model in simulator

The centrifugal compressor in the *UniSim Design*™ simulator calculates either a stream property (pressure or temperature) or compression efficiency depending on the specified information. The solution in general is a function of flow, pressure change, applied energy, and efficiency. There are two typical solution methods available for compressors, one without curves and one with. In this work, a steady-state model of centrifugal compressors is solved without a compressor curve. However, it is important to note that if compressor curves are available, they have to be considered to increase the model rigorousness. In the case without compressor curves, the *Unisim Design*™ calculates the required energy, outlet temperature and other efficiency by using Eqs. (4)–(7) [21] for a given flow rate, inlet temperature, inlet-outlet pressures and isentropic or polytropic efficiencies. The isentropic and polytropic efficiency of the compressor (represented by Eqs. (4) and (5)) in the *Unisim Design*™ are based on the work of Schultz [24].

The isentropic and polytropic efficiencies are:

$$\eta_{\text{isentropic}} = \frac{W_{\text{isentropic}}}{W_{\text{actual}}} \tag{4}$$

$$\eta_{\text{polytropic}} = \frac{\left[\left(\frac{P_{\text{out}}}{P_{\text{in}}}\right)^{\left(\frac{n-1}{n}\right)} - 1\right] \times \left[\left(\frac{n}{n-1}\right) \times \left(\frac{k-1}{k}\right)\right]}{\left(\frac{P_{\text{out}}}{P_{\text{in}}}\right)^{\left(\frac{k-1}{k}\right)}} \times \eta_{\text{isentropic}} \tag{5}$$

where the polytropic exponent (n) and isentropic exponent (k) are:

$$n = \frac{\log\left(\frac{P_{\text{out}}}{P_{\text{in}}}\right)}{\log\left(\frac{\rho_{\text{out,actual}}}{\rho_{\text{in}}}\right)};\quad k = \frac{\log\left(\frac{P_{\text{out}}}{P_{\text{in}}}\right)}{\log\left(\frac{\rho_{\text{out,ideal}}}{\rho_{\text{in}}}\right)} \tag{6}$$

The actual power required is equivalent to the enthalpy difference between the inlet and outlet streams:

$$W_{\text{actual}} = m'(h_{\text{outlet}} - h_{\text{inlet}}) \tag{7}$$

In this study, the compressor isentropic efficiency is set at 75% based on normal industrial experience, and 100% mechanical efficiency (i.e., no friction loss in shaft work) is assumed as in [23]. The *Unisim Design*™ performs rigorous calculations of the isentropic power by following the isentropic line from the inlet to the outlet pressure. The actual power is then calculated by dividing the ideal power by the specified compressor efficiency. The outlet temperature is then rigorously determined from the outlet enthalpy of the gas. Notice that all the intensive quantities are determined thermodynamically, using the specified property package. Once the compressor calculations are completed, the adiabatic and polytropic heads are performed based on the ASME method [24].

3.5. Simulation basis and optimizing variables

The feed conditions used to develop SMR plant are listed in Table 1. The Peng-Robinson equation of state was used to calculate the thermodynamic properties. The MITA of the LNG heat exchanger was set at 3 °C. Furthermore, 8% of the NG was considered to be converted to boil-off gas after the sub-cooled LNG is flashed to atmospheric pressure.

The key decision variables that affect the overall operational performance of the SMR process are the MR's suction and condensation pressure, MR flow rate and composition, and extent of MR vaporization. The extent of MR vaporization affects the overall approach temperature of the LNG exchanger, and consequently, the thermodynamic feasibility of heat transfer. While including it in the optimizing variables restricts the solution to a feasible domain and has very little effect on compressor power minimization. Increase of suction and condensation pressure induces higher irreversibility in the SMR plant by increasing the temperature differential between the composite curves, and leads to greater demands on compressor work. At the same time, MR composition also affects the compression power requirement and the feasibility of the heat exchanger. The lower boiling component in MR for instance, nitrogen imparts a refrigeration effect that is visible at the cold end of composite curves, and a higher boiling MR component provides refrigeration that is visible in the warm end of composite curves. An optimum refrigerant mixture provides nearly reversible operation of the LNG plant by bringing composite curves with MITA apart, subsequently reducing the compression power

Table 1
Feed conditions and simulation assumptions.

Property	Condition
NG temperature	32 °C
NG pressure	50 bar
NG flow rate	1.0 kg/hr
NG composition (mole fraction)	
N_2	0.002000
CH_4	0.913483
C_2H_6	0.053611
C_3H_8	0.021404
n-C_4H_{10}	0.004701
i-C_4H_{10}	0.004601
n-C_5H_{12}	0.000100
i-C_5H_{12}	0.000100
Compressor isentropic efficiency	0.75
MR temperature after cooler	40 °C
MCHE pressure drop	
ΔP hot stream	1 bar
ΔP cold stream	1 bar

Author's personal copy

requirement. The MR system is highly nonlinear, and the non-simultaneous optimization of variables makes reaching a global optimum very unlikely. Considering the limitations of earlier adopted optimization approaches (see Section 1), PSP is a suitable choice, and good engineering judgments coupled with a robust optimization algorithm make attaining a global optimum very likely. These optimizing variables need specific constraints related to their physical nature.

4. SMR process optimization

4.1. Base case and variable limits

The key decision variables in the SMR process design are listed in Table 2. The base case for optimization was selected by mesh searching or Brute force method. This time-consuming and exhaustive search method selected a basic feasible solution – the base case – using a suitable degree of mesh coarseness. Through engineering judgment and following the hardware constraints the upper limit and lower limit for optimizing variables were selected as 30% higher and lower value of base case.

4.2. Composite curves

The interactions between the decision variables can be represented in a single set of composite curves (CCs) that also help to validate the heat transfer. The curves should be close to each other and at least MITA apart. The lower bound CCs (Fig. 3a) are almost overlapping (lower power consumption) and the upper bound CCs (Fig. 3b) are well separated (higher power consumption). The optimal CCs lie within these bounds and will be sought during optimization.

4.3. Objective function and constraints

LNG plant design invites large costs in terms of operational and capital. The minimizations of operational and capital cost often conflict with each other. The reason is that minimizing capital cost needs small heat transfer area that leads to greater demand on compressor work consequently on operational cost. To resolve this problem, multi-objective optimization (MOO) [25] must be solved in designing an LNG plant. MOO is used when the problem involves two or more objectives which are often conflicting and there will be many optimal solutions known as Pareto-optimal. Pareto-optimal optimization [26] is particularly useful for solving multi-objective optimization problems when moving from one point to another; one objective function improves while the other worsens. However, in this study MOO is not solved and single objective of compression energy minimization was achieved by referring the previous published approaches. The success of operational optimization of the LNG plant depends on the selection of an appropriate objective function, which has been made by considering the following

Table 2
Decision variables' limits.

Property	Base case value	Lower bound	Upper bound
N_2 mass flow (kg/hr)	0.2510	0.1506	0.3514
CH_4 mass flow (kg/hr)	0.5680	0.3408	0.7952
C_2H_6 mass flow (kg/hr)	0.5520	0.3312	0.7728
C_3H_8 mass flow (kg/hr)	2.930	1.7580	4.6880
Condenser pressure (Bar)[a]	48.00	35	52
MR temp. after expansion (°C)	−155.0	−162	−152

[a] Suction pressure kept constant and the difference in pressure is addressed by condenser pressure only.

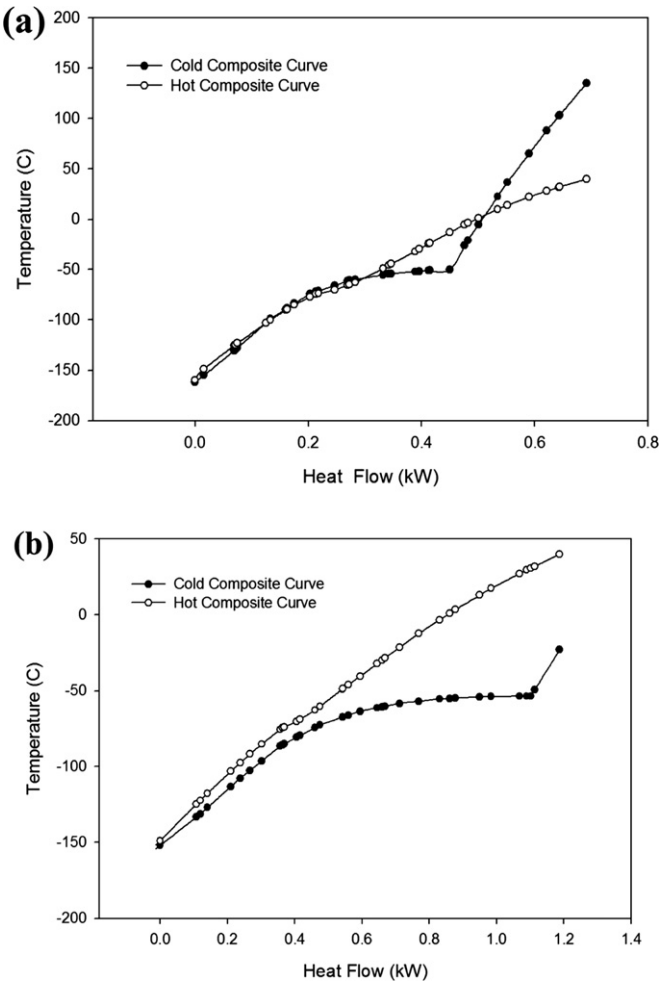

Fig. 3. Composite curves for (a) lower bound case and (b) upper bound case.

approaches. Hatcher et al. [27] considered several operational objective functions in LNG plant optimization, and it was found that minimization of the compressor power requirement created the best fit between the hot and cold composite curves, consequently leading the process toward reversibility. Wang et al. [23] also considered the minimization of compressor energy consumption as the objective of optimization in an LNG plant. In this study, the LNG plant operation is also optimized by minimizing the compressor shaft work requirement. The objective function, compression power requirement, is defined relative to the key design variables in a general form for optimization:

$$\text{Minimize } F(X) = W_S \tag{8}$$

where

$$X = \{m'_{N2}, m'_{C1}, m'_{C2}, m'_{C3}, \alpha, \mu\}' \tag{9}$$

subject to

$$h_k(X) = 0$$

$$g_k(X) < 0$$

$$X^L \le X \le X^U$$

where X is the key decision variable vector defined by Eq. (9) and m'_{N2} to m'_{C3} represent mass flows of refrigerant components. α and

Author's personal copy

μ represent the compressor suction pressure and the MR temperature after expansion, respectively. The power requirement of the compressor is denoted by *Ws*. Since the power consumption of the intercoolers is mainly due to the circulation of water though the intercoolers, which is much cheaper than that for gas compression, it can be safely neglected in the objective function. Optimizing variables include all the relevant thermodynamic and physical properties, including the bubble and dew point temperatures of the MR, the latent heats of vaporization and the specific heat of the vapor-phase mixture. There are several constraints in the proposed process that must be considered to achieve a practical solution. Constraints must be satisfied; MITA in the LNG exchanger and the degree of superheat of the MR refrigerant, that characterizes the LNG plant's thermodynamic validity and safety. The variable bounds constitute mini–max constraints. All the constraints used in this study are listed in Table 3. The complexity of the objective and constraints functions precludes parametric study of each variable's effects on the compressor power and heat exchanger load. Hence PSP is used here to assess the effects of changing the variables within their defined ranges. The PSP algorithm used here is illustrated in Fig. 1. Several parameters that determine the successful convergence of the PSP are listed in Table 4, chosen with regard to the conditions of the objective function and the constraints. The PSP source code was written in Mathworks *MATLAB*™ and connected to the *UniSim Design*™ in client/server fashion using the COM functionality. The key decision parameters were passed to the PSP optimizer, which generated the first set of decision variables and passed them back to the simulator. The process was simulated, the given objective and constraints were evaluated and a new set of decision variables were generated, and supplied back to the PSP algorithm. The procedure continued until it reached the maximum number of iterations or the global error gradient was below a specified limit.

4.4. Constraint handling in the PSP

The constraints posed by the SMR optimization problem are highly nonlinear due to their complex thermodynamic relationship. There are several methods for handling nonlinear constraints in evolutionary algorithms [28]. The augmented Lagrange penalty function method is used here; it is easy to implement and well suited to handling constraints. The constraints are folded into the objective function and the constraints problem is transformed into an unconstrained one. The form of the augmented Lagrange penalty function method [29] used here is:

$$F(\phi,\beta,r_g) : f(\phi) + r_g \sum_{j=1}^{m} \left(\max\left[\theta_j(\phi), -\frac{\beta_j}{2r_g}\right]\right)^2 + \sum_{j=1}^{m} \beta_j \left(\max\left[\theta_j(\phi), -\frac{\beta_j}{2r_g}\right]\right) \quad (10)$$

Table 3
Design constraints in SMR optimization.

Mini–max constraints on variable bounds	Design constraints
$0.1506 \le m'_{N2} \le 0.3514$ (kg/hr)	$\Delta T_{min} \ge 3$ °C
$0.3408 \le m'_{C1} \le 0.7952$ (kg/hr)	$T_{LNG} \le -157$ °C exit temperature of LNG from LNG exchanger
$0.3408 \le m'_{C2} \le 0.7728$ (kg/hr)	Degree of superheat of MR ≥ 36 °C
$1.7580 \le m'_{C3} \le 4.6880$ (kg/hr)	
$35 \le \alpha \le 52$ (Bar)	
$-162 \le \mu \le -152$ (°C)	

Table 4
PSP parameters.

PSP parameter	Value
Number of particles	30
Cognition learning parameter (c_1)	2.0
Social learning parameter (c_2)	2.1
Maximum velocity of particle (V_{max})	4.0
Inertial weight (w)	0.9 → 0.2 (linearly decreasing)

Table 5
PSP optimization results.

Objective function	PSP optimizer	Base case (Mesh search)	Unit
$J = \sum W_s$	**0.3807**	**0.4232**	kW
Decision variable	Optimized value	Initial estimate	Unit
m'_{N2}	0.2263	0.2510	kg/hr
m'_{C1}	0.4711	0.5680	kg/hr
m'_{C2}	0.5714	0.5520	kg/hr
m'_{C3}	2.769	2.930	kg/hr
α	46.50	48.00	Bar
μ	−152.7	−155.0	°C

Bold values signify the core result of this study.

where Φ = Decision variable vector, β = Multiplier associated with the inequality constraints, r_g = Penalty multiplier, $\theta_j(\phi)$ = Nonlinear constraints (see Table 3).

5. Optimization results

Using the PSP algorithm, SMR NG liquefaction process was optimized by varying the key decision variables between fixed bounds, while satisfying the constraints. The optimization results are listed in Tables 5–9. Initially there were six optimization variables, incorporating nonlinear constraints increases this to nine. The PSP optimizer also treats the Lagrange value as a variable to be optimized and looks for the best solution within the search space. The convergence of PSP algorithm is shown in Fig. 6. The rigor of the final solution can be attributed to the computational cost, which is quite high when the PSP is used in the optimization-simulation framework. A compression energy saving of 10.04% and exergy efficiency improvement of 5% (see Table 8) was achieved compared with the base case. The optimization results can be physically interpreted in the CCs shown in Fig. 4a and b. In Fig. 4a, the base case CCs have a gap of more than 3 °C in the temperature range of −160 °C to −50 °C. Refrigeration is quite expensive at low temperatures, and bringing this gap closer makes heat transfer more efficient, and brings the system to reversible operation. This gap represents room for improvement by the PSP optimizer. The improvement is visible in the optimized case CCs (Fig. 4b), where the CC are approaching more closely to MITA criterion from the −160 °C to −50 °C temperature range. The horizontal length of the CC or the heat flow value in Fig. 3 is represented on the *x*-axis, and has units of (kW). This length is closely related to the compression energy consumption. The optimized CCs have horizontal length values of 0.85 kW, and the base case CCs have 0.9 kW. The decrease of 0.04 kW provides validation for the success of PSP optimization. Similarly, Fig. 5 represents the variation of approach temperature

Table 6
Optimized LNG exchanger performance.

Performance parameter	Numerical value
Overall heat transfer coefficient	509.73 kJ/C-h
Log mean temperature difference	6.937 °C
Duty	3.105e+03 kJ/h

Author's personal copy

Table 7
Details of compression work.

Compression stage	Pressure (bar)		Power required (kW)
	Inlet	Outlet	
Stage 1	1.000	2.611	0.10307
Stage 2	2.611	6.818	0.10117
Stage 3	6.818	17.80	0.09523
Stage 4	17.80	46.50	0.08137

Table 8
Exergy efficiency analysis.

System	Exergy efficiency (%)	
	Base case	Optimized case
Compressor & cooler assembly	41.96	42.47
LNG exchanger	58.19	69.72
Whole process	45.64	50.77

within the heat exchanger. The optimum approach temperature in optimized case is more close to 3 °C in the cold end and proves the success of optimization.

Comparison between the PSP-optimized results and the previous approaches is summarized in Table 9: PSP was successful in finding the values of optimizing variables that ensures a close temperature approach between the hot and cold streams over the entire length of heat exchanger, at reduced overall system pressure, resulting in improved energy efficiency. The saving of about 7.7% energy in comparison with the PRICO™ process and 10% compared with the base case and the NLP optimized case [11] was achieved. The optimal solution reported by Khan et al. is the result of an NLP optimization study. The operational design problem of SMR liquefaction is likely to have many local optima as already stated. Traditional deterministic optimization methods would become readily trapped in them. At the same time, the stochastic optimization methods offer more confidence in the optimality of the final solution at the expense of computational time. Being stochastic in nature, the PSP outperforms NLP optimization, and the results in Table 9 validate this. Although the PSP helps in getting better results at the expense of computation cost, it still does not guarantee global optimum.

6. Exergy efficiency analysis

Exergy (E) is the potential of a system to cause a change as it achieves equilibrium with its environment through a hypothetical reversible process [30]. In other words, the exergy of a system with a given set of chemicals represents the maximum potential work that the system can produce if it is reversibly brought into a state of thermodynamic equilibrium with the environment [31]. For calculating the exergy of a stream of matter, the exergy can be divided individually into different components. In the absence of nuclear effects, magnetism, electricity and surface tension, exergy and change in exergy can be calculated by Eqs. (11) and (12).

Table 9
Comparison of specific power requirement from previous studies.

Case	Commercial PRICO™ process [3]	Aspenlund et al. [12]	Khan et al. [11]	PSP optimized
Specific power (kJ/kg LNG)	1485.0	1444	1527.8	1370.0
MITA	–	2.93 °C	3.0 °C	3.0 °C

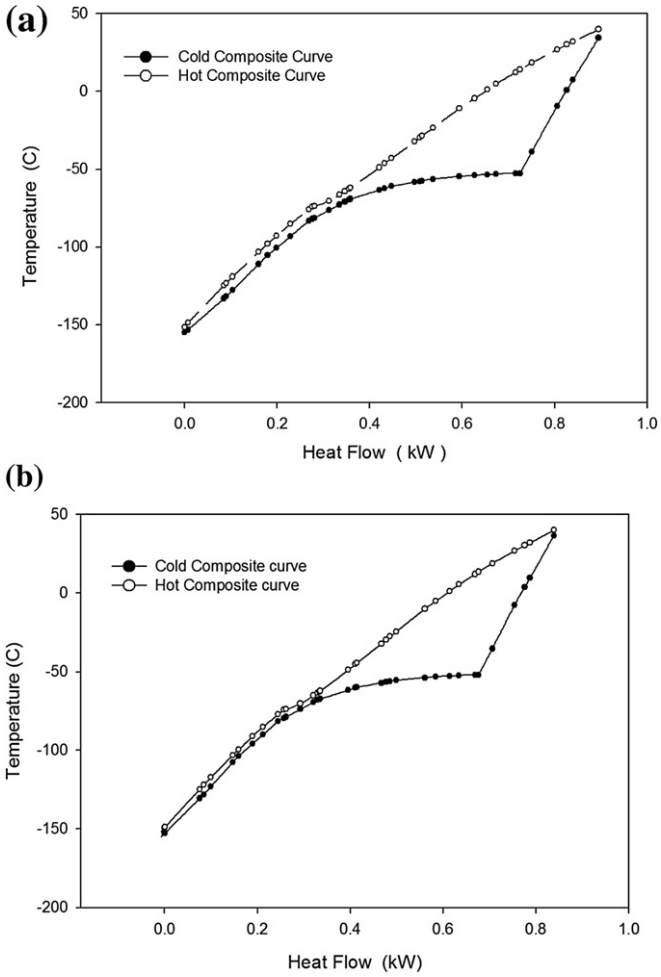

Fig. 4. Composite curves for (a) base case and (b) PSP optimized case.

$$E = E_k + E_p + E_{\text{phy}} + E_{\text{chem}} \tag{11}$$

$$\Delta E = (H - H_o) - T_o(S - S_o) + \frac{\text{Vel}^2 - \text{Vel}_o^2}{2} + mg(Z_1 - Z_2) \tag{12}$$

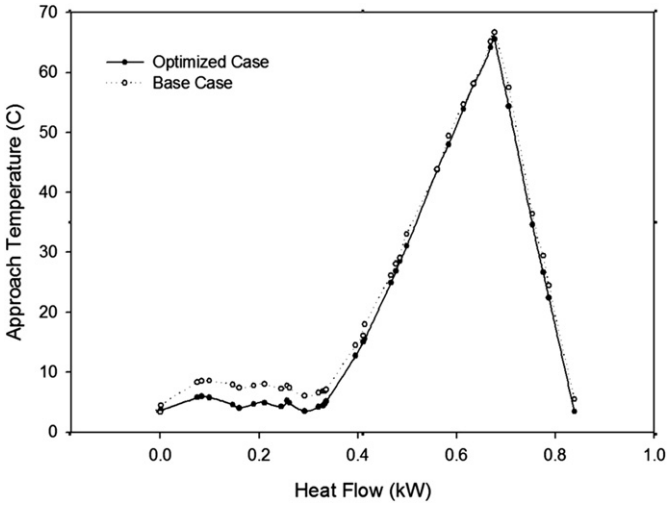

Fig. 5. Approach temperature variation within a heat exchanger.

Author's personal copy

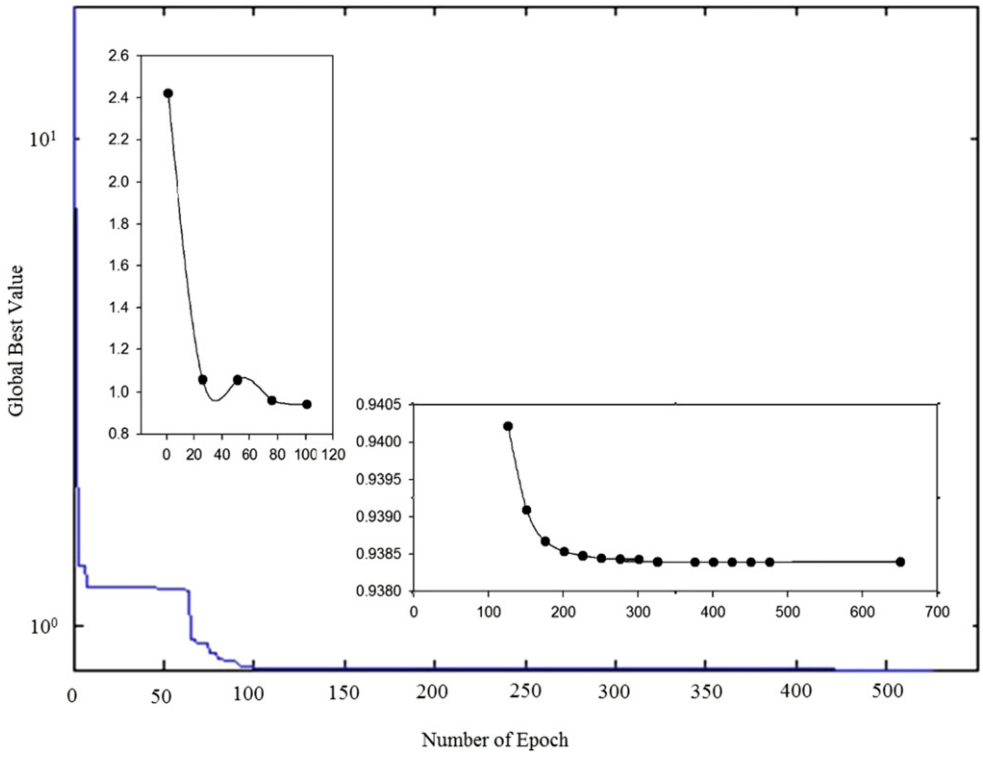

Fig. 6. Convergence of the PSP.

where E_k, E_p, E_{phy} and E_{chem} are the kinetic, potential, physical and chemical exergy, respectively. Since the system under study does not include chemical reactions, mixing and separation, E_{chem} can be safely ignored. At the same time the mechanical exergy (E_k and E_p) is small in comparison to the physical exergy (temperature and pressure based exergy) and hence ignored in calculations [32].

Extending the above concept, the expression for work required for cooling/liquefying a stream of gas with flow rate m' as shown in Fig. 7 is given by

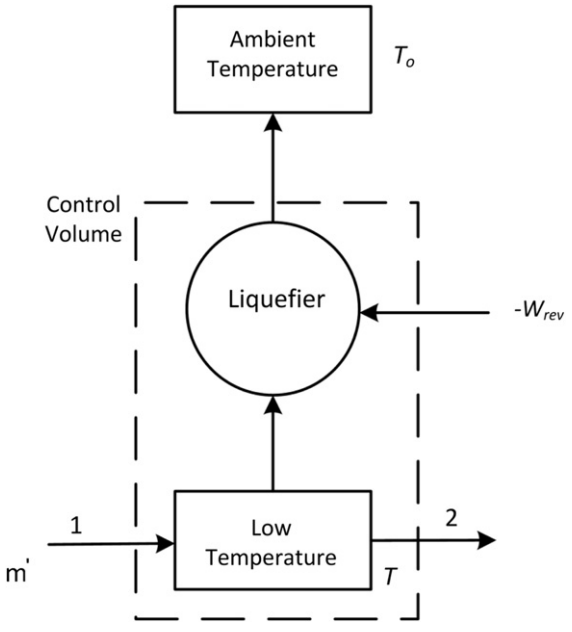

Fig. 7. Reversible gas cooler/liquefier.

$$-W_{rev} = m'[(h_1 - h_2) - T_o(s_1 - s_2)] = m'(ex_1 - ex_2) \quad (13)$$

which corresponds to the exergy loss of the individual unit operation. The exergy efficiency is defined by

$$\eta_{ex} = 1 - \frac{\sum \text{exergy destructed in each component}}{\text{actual power supplied}} \quad (14)$$

The benefit of exergy calculations in thermodynamic systems like natural gas liquefaction has many folds. It gives an idea of deviation from ideal state and also enables determination of the location, type and true magnitude of losses. Once natural gas is liquefied, the cryogenic exergy of LNG can be utilized in many ways, such as air separation, power cycle [33] material freezing, and electricity generation etc. Szarhut et al. [34] utilized the cryogenic exergy of LNG with reduced environment emissions without carrying out combustion of NG.

Based on the Eqs. (11)–(14), the exergy efficiency analysis [35] was carried out and reported in Table 8. It can be seen that exergy efficiency of LNG exchanger after optimization has increase by about 11% and that of the whole process by 5%. The increase of LNG exchanger efficiency is attributed to the near optimum heat transfer and close matching of composite curves. The major irreversibility of the process is associated with the compression and cooler assembly which has exergy efficiency of about 42% in optimized case. More efforts are needed for optimizing the compression assembly and will be reported in the future work.

7. Conclusions

SMR NG liquefaction process was optimized to reduce compression energy requirement using the PSP algorithm. The constraints were folded into the objective function using the augmented Lagrange penalty function. The PSP is successful in finding the values of optimizing variables that ensures a close

Author's personal copy

temperature approach between the hot and cold streams over the entire length of heat exchanger, at reduced overall system pressure, resulting in improved exergy efficiency. The saving of about 7.7% energy in comparison with the PRICO™ process and 10% compared with the base case and the NLP optimized case is achieved. The main advantage of the PSP lies in the fact that no initial guess is needed to start the optimization, while traditional deterministic optimization methods can easily become trapped in local optima. The stochastic features of PSP give more confidence in the optimality of its final solution. This method works in an optimization-simulation framework, process model built in a commercial simulator able to be directly optimized with reduced effort.

Acknowledgment

This research was supported by a grant from the gas plant R&D center funded by the Ministry of Land, Transport & Maritime Affairs (MTLM) of the Korean Government.

References

[1] Finn AJ. Are floating LNG facilities viable options? HC Engineering; July 2009. p. 31–8.
[2] Khalilpour R, Karimi IA. Evaluation of utilization alternatives for stranded natural gas. Energy 2012;40:317–28.
[3] Remeljej CW, Hoadley AFA. An exergy analysis of small-scale liquefied natural gas (LNG) liquefaction processes. Energy 2006;31(12):2005–19.
[4] Ait-Ali MA. Optimal mixed refrigerant liquefaction of natural gas. Ph.D. dissertation, Mechanical Engineering Department, Stanford University, CA; 1979.
[5] Duvedi A, Achenie LEK. On the design of environmentally benign refrigerant mixtures: a mathematical programming approach. Comp Chem Eng 1997; 21(8):915–23.
[6] Churi N, Achenie LEK. The optimal design of refrigerant mixtures for a two-evaporator refrigeration system. Comp Chem Eng 1997;21:S349–54.
[7] Vaidyaraman S, Maranas CD. Synthesis of mixed refrigerant cascade cycles. Chem Eng Commun 2002;189(8):1057–78.
[8] Lee GC, Smith R, Zhu XX. Optimal synthesis of mixed-refrigerant systems for low-temperature processes. Ind Eng Chem Res 2002;41:5016–28.
[9] Mokarizadeh HSM, Mowla D. Energy optimization for liquefaction process of natural gas in peak shaving plant. Energy 2010;35:2878–85.
[10] Nogal FD, Kim JK, Perry S, Smith R. Optimal design of mixed refrigerant cycles. Ind Eng Chem Res 2008;47:8724–40.
[11] Khan MS, Lee S, Lee M. Optimization of single mixed refrigerant natural gas liquefaction plant with nonlinear programming. Asia-Pac J Chem Eng 2012; 7(S1):62–70.
[12] Aspenlund A, Gunddersen T, Myklebust J, Nowak MP, Tomasgard A. An optimization-simulation model for a simple LNG process. Comp Chem Eng 2010;34:1606–17.
[13] Kennedy J, Eberhart RC. Particle swarm optimization. In: Proceeding of the IEEE international conference on evolutionary computation. Piscataway, NJ: IEEE Press.; 1998. p. 69–73.
[14] Eberhart RC, Hu X. Human tremor analysis using particle swarm optimization. In: Proceedings of IEEE congress on evolutionary computation 1999. Piscataway, NJ. Washington, DC: IEEE Press; 1999. p. 1927–30.
[15] Tandon V. Closing the gap between CAD/CAM and optimized CNC end milling, Master's thesis, Purdue School of Engineering and Technology, Indiana University Purdue University Indianapolis, USA; 2000.
[16] Yoshida H, Kawata K, Fukuyama Y, Nakanishi Y. A particle swarm optimization for reactive power and voltage control considering voltage stability. In: Torres GL, Alves da Silva AP, editors. Proceeding. International. Conference on intelligent system application to power systems, Rio de Janeiro, Brazil; 1999. p. 117–21.
[17] Soares J, Silva M, Sousa T, Vale Z, Morais H. Distributed energy resource short-term scheduling using signaled particle swarm optimization. Energy 2012;44: 466–76.
[18] Siddhartha, Sharma N, Varun. A particle swarm optimization algorithm for optimization of thermal performance of a smooth flat solar air heater. Energy 2012;38:406–13.
[19] Eberhart RC, Shi Y. Particle swarm optimization: developments, applications and resources. In: Proceedings congress on evolutionary computation 2001, Seoul, Korea, vol. 1; 2001. p. 81–6.
[20] Geist JM. The role of LNG in energy supply. Int J Refrig 1983;6(5):283–97.
[21] Honeywell™, OLIPro operation manual guide; 2007. NJ, USA.
[22] Hasan MM, Karimi IA, Alfadala HE, Grootjans H. Operational modeling of multistream heat exchangers with phase changes. AIChE J 2009;55:150–71.
[23] Wang M, Zhang J, Xu Q. Optimal design and operation of a C3MR refrigeration system for natural gas liquefaction. Comp Chem Eng 2012;39:84–95.
[24] Schultz JM. The polytropic analysis of centrifugal compressors. J Eng Power 1962:69–82.
[25] Kusiak A, Xu G, Tang F. Optimization of an HVAC system with a strength multi-objective particle-swarm algorithm. Energy 2011;36:5935–43.
[26] Shah NM, Hoadley AFA, Rangaiah GP. Inherent safety analysis of a propane pre-cooled gas-phase LNG process. Ind Eng Chem Res 2009;48:4917–27.
[27] Hatcher P, Khalilpour R, Abbas A. Optimisation of LNG mixed-refrigerant processes considering operation and design objectives. Comp Chem Eng 2012;41:123–33.
[28] Mezura-Montes Efren. Constraint-handling in evolutionary optimization. 1st ed. New York, USA: Springer; 2009.
[29] Venkataraman P. Applied optimization with MATLAB® programming. 2nd ed. New York, USA: Wiley; 2009.
[30] Sato N. Chemical energy and exergy. 1st ed. Amsterdam, Netherlands: Elsevier; 2004.
[31] Zhang J, Xu Q. Cascade refrigeration system synthesis based on exergy analysis. Comp Chem Eng 2011;35:1901–14.
[32] Aspelund A, Berstad DO, Gundersen T. An extended pinch analysis and design procedure utilizing pressure based exergy for subambient cooling. Appl Therm Eng 2007;27:2633–49.
[33] Liu Y, Guo K. A novel cryogenic power cycle for LNG cold energy recovery. Energy 2011;36:2828–33.
[34] Szarhut J, Szczygiel I. Utilization of the cryogenic exergy of liquid natural gas (LNG) for the production of electricity. Energy 2009;34:827–37.
[35] Venkatarathnam G. Cryogenic mixed refrigerant processes. 1st ed. New York, USA: Springer; 2008.

Nomenclature

Parameters and variables

ASME: American society of mechanical engineers
CCs: composite curves
COM: component object model
JT: Joule Thompson
LNG: liquefied natural gas
MINLP: mixed integer nonlinear programming
MITA: minimum internal temperature approach
MR: mixed refrigerant
MOO: multi-objective optimization
NG: natural gas
NLP: nonlinear programming
PSP: particle swarm paradigm
SMR: single mixed refrigerant
UA: overall heat transfer coefficient
c_1: cognition learning parameter
c_2: social learning parameter
E: exergy
ΔE: exergy difference
E_k: kinetic exergy
E_p: potential exergy
E_{phy}: physical exergy
E_{chem}: chemical exergy
ex_1: specific exergy of stream 1 in Fig. 7
ex_2: specific exergy of stream 2 in Fig. 7
g: gravitational acceleration
g_{Best}: global best location
g_k: inequality constraints
h_k: equality constraints
h_1: specific enthalpy of stream 1 in Fig. 7
h_2: specific enthalpy of stream 2 in Fig. 7
h_{outlet}: specific enthalpy of compressor outlet stream
h_{inlet}: specific enthalpy of compressor inlet stream
h_{in}: specific enthalpy at inlet layer in LNG exchanger
h_{out}: specific enthalpy at outlet layer in LNG exchanger
H: enthalpy
H_o: enthalpy at ambient temperature
k: isentropic exponent
m: mass of the system
$\dot{m}$: mass flow rate
$\dot{m}_{N2}$: mass flow rate of nitrogen in mixed refrigerant
$\dot{m}_{C1}$: mass flow rate of methane in mixed refrigerant
$\dot{m}_{C2}$: mass flow rate of ethane in mixed refrigerant
$\dot{m}_{C3}$: mass flow rate of propane in mixed refrigerant
n: polytropic exponent
p_{Best}: particle best location
P_{out}: outlet pressure from compressor
P_{in}: inlet pressure to compressor
Q_{int}: heat gained from surrounding layers in the LNG exchanger
Q_{ext}: heat gained from external environment in the LNG exchanger
r_1: PSP random factor one
r_2: PSP random factor two
s_1: specific entropy of stream 1 in Fig. 7
s_o: specific entropy stream 2 in Fig. 7

Author's personal copy

state-x: physical state of individual stream in SMR process
S: entropy
S_o: entropy at ambient temperature
T: temperature
T_o: ambient temperature
Vel_o: reference velocity of matter in system
Vel: velocity of matter in system
V_i: particle velocity
Vmax: maximum velocity of particle
w: inertial weight
$W_{isentropic}$: isentropic work
W_{actual}: actual work
W_{rev}: reversible work
W_s: compressor power requirement
X: decision variable vector
X^U: upper bound for decision variables
X^L: lower bound for decision variables
X_i: individual particle position in solution hyperspace
Z_1: system elevation
Z_2: reference level
ρ: gas density
α: compressor suction pressure
μ: mixed refrigerant after expansion temperature
η_{ex}: exergy efficiency
$\eta_{isentropic}$: isentropic efficiency
$\eta_{polytropic}$: polytropic efficiency